AD-A133 709 USE OF ACOUSTICS IN LOCALIZING UNDER-ICE OIL SPILLS(U) 1/1
WASHINGTON UNIV SEATTLE APPLIED PHYSICS LAB
R E FRANCOIS ET AL. AUG 83 APL-UW-8309 USCG-D-26-83
UNCLASSIFIED N00024-81-C-6042 F/G 8/12 NL

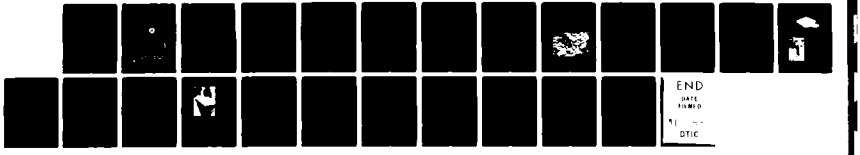

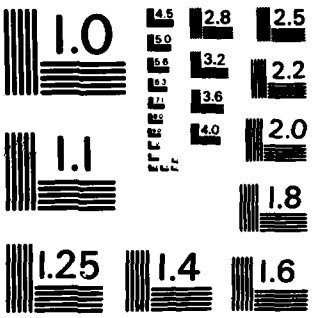

MICROCOPY RESOLUTION TEST CHART
NATIONAL BUREAU OF STANDARDS-1963-A

Report No. CG-D-26-83

USE OF ACOUSTICS IN LOCALIZING UNDER-ICE OIL SPILLS

R. E. Francois

T. Wen

Applied Physics Laboratory

University of Washington

Seattle, Washington 98105

August 1983

FINAL REPORT

Prepared for

DEPARTMENT OF TRANSPORTATION
UNITED STATES COAST GUARD
Office of Research and Development
Washington, D.C. 20593

NOTICE

Technical Report Documentation Page

1. Report No.	2. Government Accession No.	3. Recipient's Catalog No.
CG-D-26-83	AD-A133 709	

4. Title and Subtitle	5. Report Date
Use of Acoustics in Localizing Under-Ice Oil Spills	August 1983
	6. Performing Organization Code: APL-UW 8309
7. Author(s): R.E. Francois and T. Wen	8. Performing Organization Report No.
9. Performing Organization Name and Address: Applied Physics Laboratory, University of Washington, Seattle, WA 98105	10. Work Unit No. (TRAIS)
	11. Contract or Grant No.: N00024-81-C-6042
12. Sponsoring Agency Name and Address: U.S. Coast Guard, Office of Research and Development, Washington, DC 20593	13. Type of Report and Period Covered: Final Report
	14. Sponsoring Agency Code: G-DMT-3/54

15. Supplementary Notes

16. Abstract

—Because of the development of oil resources in the Arctic, it has become necessary to devise methods of dealing with accidental spills of oil beneath and near sea ice. One of the first steps involved in cleaning up an under-ice oil spill is determining its exact location. If a means of rapidly locating an under-ice oil spill can be developed, appropriate recovery techniques that capitalize on that information can then be considered. This report describes a study undertaken to determine the feasibility of using underwater acoustics to specifically locate an under-ice oil spill whose general position is known. The first step was to measure the surface backscattering strength of sea ice at 100-300 kHz at low grazing angles. The results were then used to calculate the distance at which oil spills should be detectable. The design of an operational survey system should be relatively straightforward, once the parameters of the system are defined.

17. Key Words	18. Distribution Statement
Acoustics Oilspill Detection Surface Backscattering Strength Under-ice sonar Transducer	Document is available to the public through the National Technical Information Service, Springfield, Virginia 22161

19. Security Classif. (of this report)	20. Security Classif. (of this page)	21. No. of Pages	22. Price
Unclassified	Unclassified	17	

METRIC CONVERSION FACTORS

Approximate Conversions to Metric Measures

Symbol	When You Know	Multiply by	To Find	Symbol
	LENGTH			
in	inches	*2.5	centimeters	cm
ft	feet	30	centimeters	cm
yd	yards	0.9	meters	m
mi	miles	1.6	kilometers	km
	AREA			
in^2	square inches	6.5	square centimeters	cm^2
ft^2	square feet	0.09	square meters	m^2
yd^2	square yards	0.8	square meters	m^2
mi^2	square miles	2.6	square kilometers	km^2
	acres	0.4	hectares	ha
	MASS (weight)			
oz	ounces	28	grams	g
lb	pounds	0.45	kilograms	kg
	short tons (2000 lb)	0.9	tonnes	t
	VOLUME			
tsp	teaspoons	5	milliliters	mL
Tbsp	tablespoons	15	milliliters	mL
fl oz	fluid ounces	30	milliliters	mL
c	cups	0.24	liters	l
pt	pints	0.47	liters	l
qt	quarts	0.95	liters	l
gal	gallons	3.8	liters	l
ft^3	cubic feet	0.03	cubic meters	m^3
yd^3	cubic yards	0.76	cubic meters	m^3
	TEMPERATURE (exact)			
°F	Fahrenheit temperature	5/9 (after subtracting 32)	Celsius temperature	°C

*1 in = 2.54 (exactly). For other exact conversions and more detailed tables, see NBS Misc. Publ. 286, Units of Weights and Measures, Price $2.25, SD Catalog No. C13.10:286.

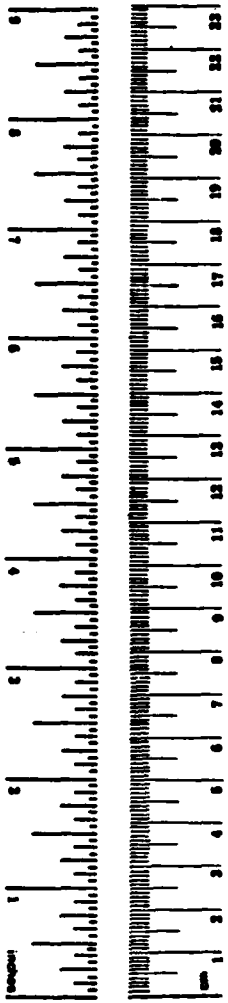

Approximate Conversions from Metric Measures

Symbol	When You Know	Multiply by	To Find	Symbol
	LENGTH			
mm	millimeters	0.04	inches	in
cm	centimeters	0.4	inches	in
m	meters	3.3	feet	ft
m	meters	1.1	yards	yd
km	kilometers	0.6	miles	mi
	AREA			
cm^2	square centimeters	0.16	square inches	in^2
m^2	square meters	1.2	square yards	yd^2
km^2	square kilometers	0.4	square miles	mi^2
ha	hectares (10,000 m^2)	2.5	acres	
	MASS (weight)			
g	grams	0.035	ounces	oz
kg	kilograms	2.2	pounds	lb
t	tonnes (1000 kg)	1.1	short tons	
	VOLUME			
mL	milliliters	0.03	fluid ounces	fl oz
l	liters	2.1	pints	pt
l	liters	1.06	quarts	qt
l	liters	0.26	gallons	gal
m^3	cubic meters	35	cubic feet	ft^3
m^3	cubic meters	1.3	cubic yards	yd^3
	TEMPERATURE (exact)			
°C	Celsius temperature	9/5 (then add 32)	Fahrenheit temperature	°F

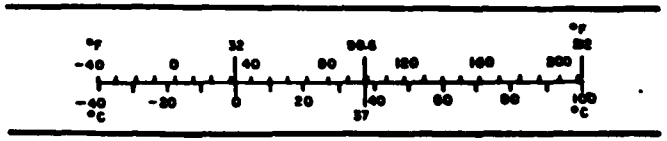

Acknowledgments

This work was supported by the Office of Research and Development, U.S. Coast Guard, Washington, D.C., under Naval Sea Systems Command contract N00024-81-C-6042. Samples of crude oil from Prudhoe Bay were provided by the ARCO refinery at Cherry Point, Ferndale, Washington. The authors wish to thank Dr. G.R. Garrison for his constructive criticism and assistance.

TABLE OF CONTENTS

LIST OF FIGURES

I. INTRODUCTION

Because of the development of oil resources in the Arctic, it has become necessary to devise methods of dealing with accidental spills of oil beneath and near sea ice. One of the first steps involved in cleaning up an under-ice oil spill is determining its exact location. If a means of rapidly locating an under-ice oil spill can be developed, appropriate recovery techniques that capitalize on that information can then be considered. At the request of the U.S. Coast Guard, the Applied Physics Laboratory undertook a study to determine the feasibility of using underwater acoustics to locate under-ice oil spills. That study, which is summarized here, concentrated on the problem of localizing an under-ice oil spill whose general position is known. First we measured the surface backscattering strength of sea ice at 100-300 kHz at low grazing angles. We then used the results to calculate the distance at which oil spills should be detectable.

II. SUMMARY

At low grazing angles, acoustic backscatter from the relatively rough ice-water interface should be substantially larger than that from the smooth oil-water interface. To obtain quantitative data on this difference, we conducted experimental investigations, in both the laboratory and the field, to determine the backscattering strength of flat sea ice in the frequency range of f = 100-300 kHz, and for grazing angles of $\theta = 10°\text{-}45°$.

The surface backscattering strength, S_S, was found to be

$$S_S = -72 + 25 \log f + 15 \log \sin \theta, \quad \text{dB},$$

with a standard deviation of 5.25 dB.

The backscatter from an oil layer under ice was too small to be measured at small grazing angles with our system.

Using the empirical formula of Eq. (1),* a sample calculation was made which showed that an under-ice sonar could effectively map the location of spilled oil under ice in an area several hundred meters in diameter. The required resolution, range, and display tradeoffs have yet to be calculated, but the necessary acoustic design information has been obtained.

*See p. 4.

III. BACKGROUND

Sea ice is a very inhomogeneous material. Freezing starts at the sea surface with small disk-shaped particles (platelets) which grow in a snowflake-like pattern; the perpendicular line through the center of the disk is the "C" axis of the ice crystal. These particles initially float with their C axis vertical. As freezing continues and the crystals begin to crowd each other, they eventually tip so that the C axis becomes horizontal. In the process, brine is concentrated between the platelets. The freezing process continues with the downward growth of the ice platelets, the eventual freezing up of the space between the platelets, and the displacement and some entrapment of the brine concentrate. We have developed a casting technique that allows us to make accurate impressions of the ice surface, or "skeletal layer." This layer is typically 2 or 3 cm deep and is quite fragile. Figure 1 is a photograph of a casting taken from a sample under-ice skeletal layer. The platelets are about 0.8 mm apart.

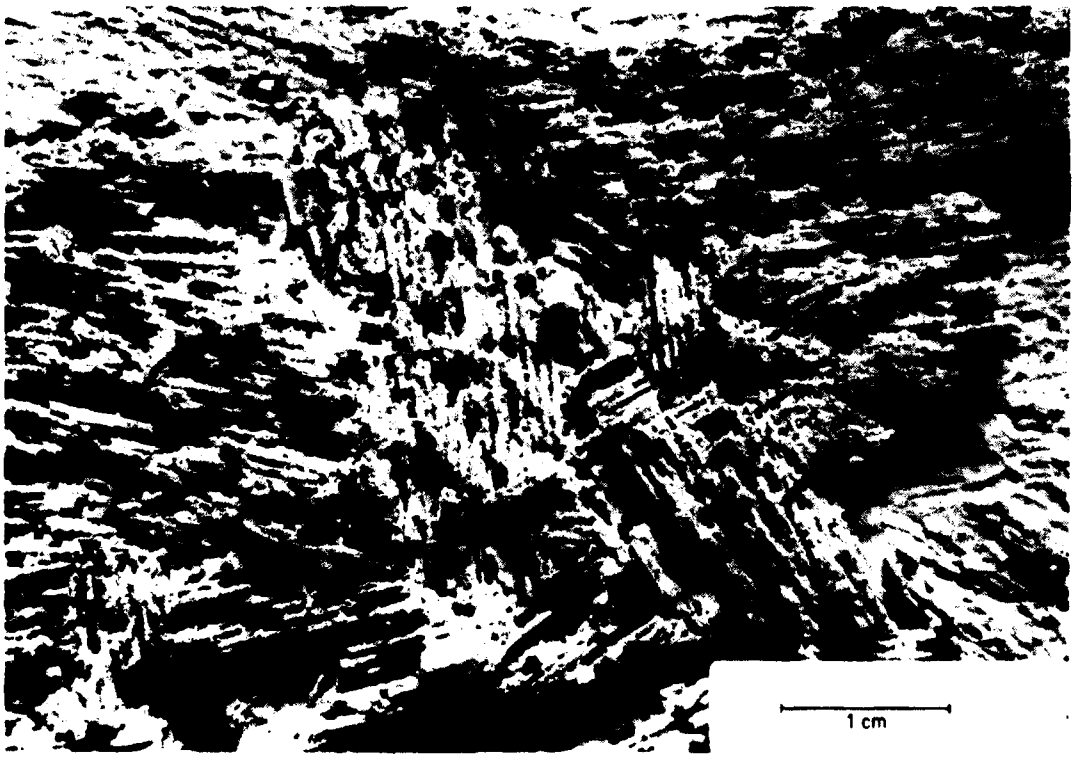

Figure 1. A casting of the under-ice skeletal layer.

The dispersion characteristics of oil that is spilled under sea ice have been extensively studied. Experiments by the U.S. Coast Guard[1,2] in the early '70s provided an excellent background for the more definitive experiments and studies that were sponsored by the Department of the Environment, Canada, in conjunction with the Beaufort Sea Project.[3-6] An excellent summary of this knowledge was given by Lewis[7] in 1976.

Oil that collects at the ice-water interface is always less dense than seawater. If the underside of the ice is perfectly flat, the oil disperses horizontally under gravitational force until an equilibrium thickness of slightly less than a centimeter is reached. The ice-water interface, however, is generally not flat. Small-scale relief in the under-ice surface is usually related to the insulating effects of the varying depths of snow cover. In the spring, the amplitude of the resulting undulations can easily be 20 to 30 cm with wavelengths of 5 to 10 m, corresponding to snow drift characteristics. Oil will thus tend to collect in pools.

Consider the case of oil spilled under ice during the freezing season. As the oil lies against the ice it impedes the flow of heat through the ice from the water to the air. Because oil has a thermal conductivity about one-fifteenth that of sea ice, its presence reduces the temperature gradient previously existing in the ice, as shown in Figure 2.

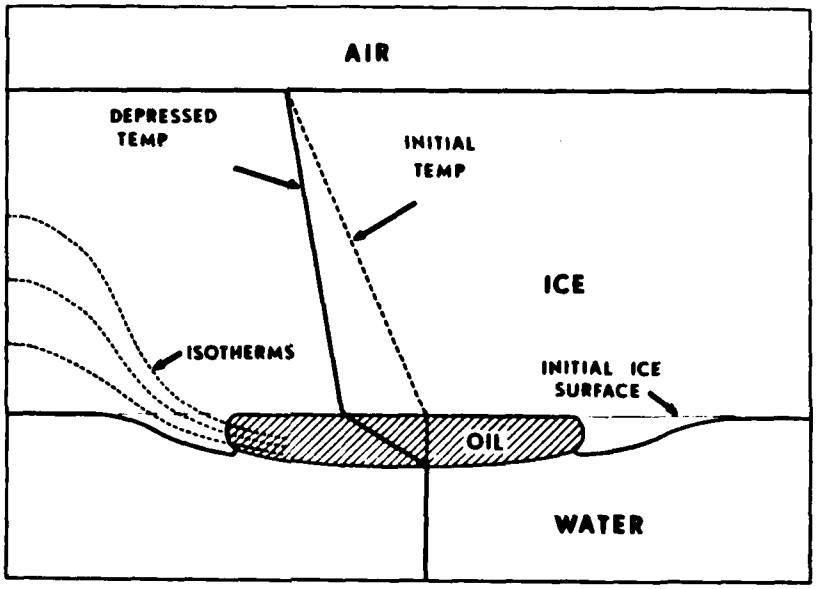

Figure 2. Effect of an oil layer beneath the ice on the freezing process.

Because the rate of heat transfer is fastest at the edge of the oil pool, a lip of ice builds up which further restrains the horizontal movement of the oil. Eventually, a new layer of ice begins to form on the lower surface of the oil, and the oil becomes encapsulated in the sea ice. The time required for encapsulation depends on ice thickness, air temperature, and oil pool thickness. In the NORCO tests,[3] this period varied from about 5 days in the fall to 10 days in the spring. The time limit for localizing and recovering the oil before it is encapsulated is therefore short during the freezing season. (During the melt season, the oil tends to rise through the brine channels created in the ice by the freezing process, resulting in collection problems different from those in other seasons.)

The idealized, or assumed, picture of an under-ice oil spill therefore is a patch of oil with a smooth, flat surface surrounded by ice of relatively rough texture. The feasibility of locating the oil acoustically depends on there being significant backscatter from the sea ice around the oil patch, in order to define its boundaries. This is analogous to the usual radar piloting problem of identifying navigable water (the area with no return signals) as opposed to the shoreline, buoys, etc. (the areas with strong return signals).

The localization system would consist of an acoustic transducer below the ice-water interface, which would directionally transmit and receive pulses in such a way as to create a plan view map of the local area. The map, analogous to a radar display, would show darkness in regions of low reflectivity, presumably the oil pool, whereas areas with high-level returns (brightness) would indicate regions of sea ice.

IV. CALCULATION OF SURFACE BACKSCATTERING STRENGTH

The parameter that characterizes the backscattering properties of a surface is called the surface scattering strength, S_s. Using Urick's[8] notation, S_s is related to other variables by

$$RL = SL - 40 \log r - 2\alpha r + S_s + 10 \log A, \quad dB//\mu Pa, \qquad (1)$$

where

RL is the received level (dB//μPa)
$= 20 \log V_r - S_x$, where

V_r = received voltage
S_x = receiving sensitivity (dB//V/μPa)

SL is the source level of the acoustic projector (dB//μPa @ 1 m)
$= 20 \log V_t + T_v$, where

V_t = transmitted voltage
T_v = transmitting sensitivity (dB//μPa/V @ 1 m)

r is the range (m)

α is the absorption coefficient (dB/m)

A is the equivalent area from which the signal is returned during a short time interval (m^2)

$$= r \Phi \frac{c\tau}{2 \cos \theta} \qquad (2)$$

for short acoustic pulses and small grazing angles, where

Φ = equivalent ideal full horizontal beam width (radians) for uniform two-way response[8]

c = velocity of sound in water (m/s)

τ = pulse length (s)

θ = grazing angle (deg).

Equation (2) can also be rewritten as

$$10 \log A = 10 \log r + 10 \log \Phi + 10 \log \frac{c\tau}{2 \cos \theta} . \qquad (3)$$

Substituting (3) into (1), we obtain

$$RL = SL - 30 \log r - 2\alpha r + S_S + 10 \log \Phi + 10 \log \frac{c\tau}{2 \cos \theta} . \qquad (4)$$

We then solve (4) for S_S:

$$S_S = RL - SL + 30 \log r + 2\alpha r - 10 \log \Phi - 10 \log \frac{c\tau}{2 \cos \theta} . \qquad (5)$$

The surface scattering strength is determined experimentally from measurements of the quantities in Eq. (5).

V. EXPERIMENTAL METHODS

A transducer was designed to measure backscatter from the under-ice surface over a wide frequency range. It consisted of a 22 × 22 element array cut from an 8.26 cm square ceramic plate (Figure 3). The elements of the center 4 × 4 array were electrically connected to a common lead, as were those of each successive row grouped around the center array, resulting in 10 electrical leads (plus a common back-plane connection) which could be combined in various ways to obtain different transducer operating characteristics. The assembled transducer, potted in polyurethane and mounted on a test fixture, is shown in Figure 4.

The transducer could be operated in either of two modes:

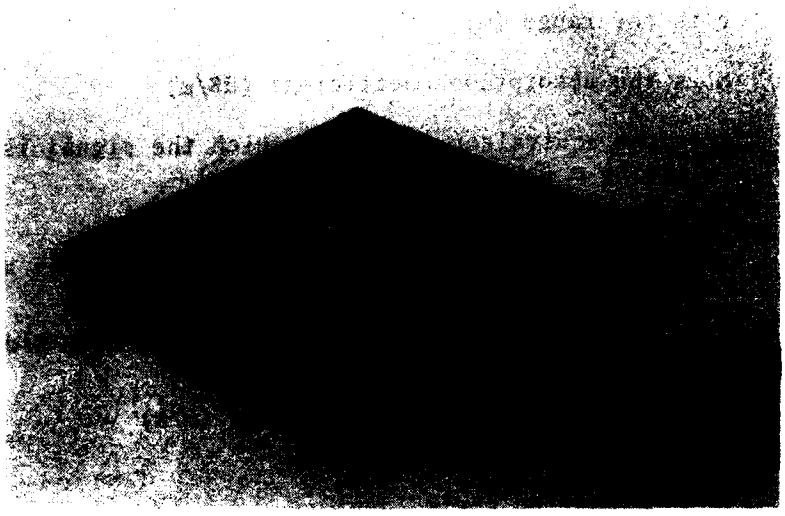

Figure 3. Array transducer of 22 × 22 elements used for backscattering measurements.

Figure 4.

Transducer assembled and mounted on the movable arm. The electrical leads are brought out through a rubber tube.

(1) Starting with the 4 × 4 array in the center, more and more squares of elements could be summed to form larger arrays. For each array, a frequency could be selected such that the beam had a particular width so that the beamwidth could be held constant regardless of which array was used. In this mode, however, the beams had relatively large side lobes.

(2) All 22 × 22 elements could be used, with proper shading, to produce beam patterns with suppressed side lobes. The width of the beam was, however, different at different frequencies.

Mode 2 was used because side lobe suppression was highly desirable, considering the confined space for our laboratory experiments. The beam width as a function of frequency for this mode is shown in Figure 5. For reasons of azimuthal resolution, relatively narrow beams should be used. Therefore only frequencies of 100, 145, 200, and 300 kHz were employed. The beam patterns at these frequencies are shown in Figure 6.

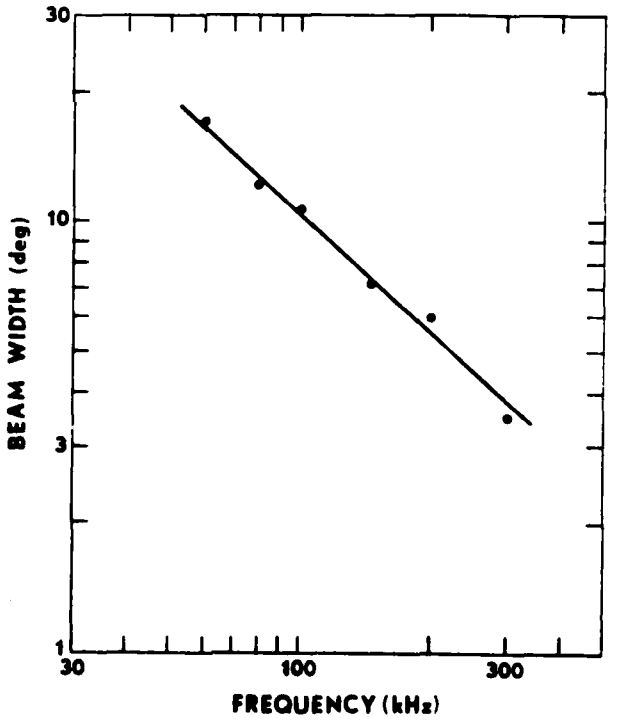

Figure 5. Variation in beam width of shaded 22 × 22 element transducer.

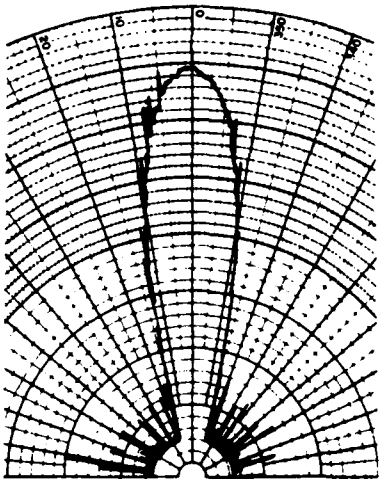

100 kHz
(noise spikes on pattern)
T_v = 150 dB//µPa/V @ 1 m
S_x = -154 dB//V/µPa

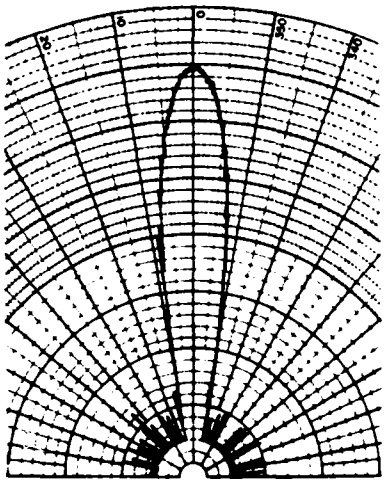

145 kHz
T_v = 157 dB//µPa/V @ 1 m
S_x = -152 dB//V/µPa

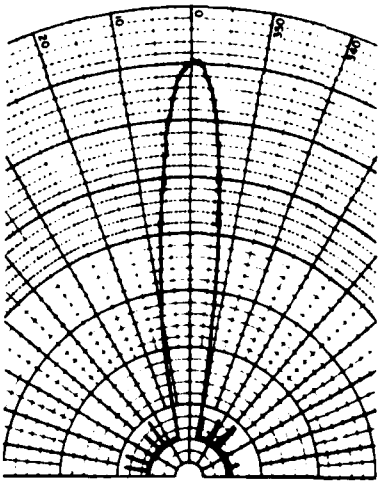

200 kHz
T_v = 171 dB//µPa/V @ 1 m
S_x = -149 dB//V/µPa

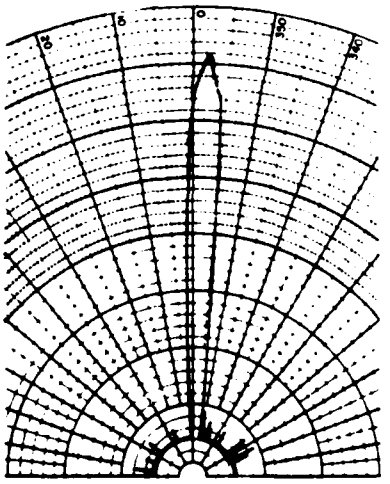

300 kHz
T_v = 162 dB//µPa/V @ 1 m
S_x = -154 dB//V/µPa

Figure 6. Beam patterns of shaded 22 × 22 element transducer (horizontal and vertical sections are the same).

In the laboratory, testing took place in an 81 cm wide × 180 cm long × 117 cm deep insulated tank in a temperature-controlled cold room. The tank was filled with salt water at 32‰ salinity. The transducer was mounted on a circular track which was positioned so that the center of the acoustic beam intercepted the ice-water interface at the same point, regardless of grazing angle. The entrance hole was sawed through the ice after the desired ice thickness was reached. A schematic of the experimental setup is shown in Figure 7, and a photograph of the tank in the cold room is shown in Figure 8.

The ice was frozen at different rates to simulate the freezing rates that would be experienced during different arctic seasons. The formation of a skeletal layer was observed in all cases. For each case, backscatter from the ice was measured at grazing angles of 10°, 15°, 20°, 30°, and 45°. At each angle, 80 μs long pulses were transmitted at 100, 145, 200, and 300 kHz. The backscattered signals were acquired and stored by a Nicolet digital oscilloscope on floppy diskettes, and later recalled for analysis.

The measurement process was repeated on an arctic field trip to the Beaufort Sea in October and November 1982. The same transducer was used as before but the grazing angle was adjusted with a parallelogram linkage. The transducer was 3 m below water level and looked upward at 60 cm thick ice. The ensonified area was substantially larger than that in the laboratory tests. Measurements were made in two arbitrarily selected directions, about 60° apart in azimuth.

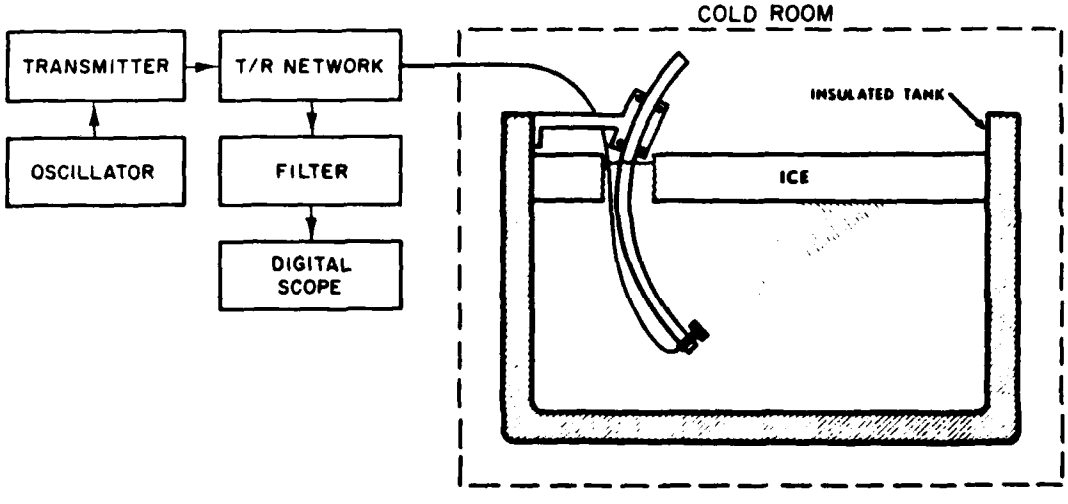

Figure 7. Block diagram of experimental setup for laboratory measurement of ice backscatter.

Figure 8.
Test tank, 0.8 × 1.8 × 1.2 m, in cold room.

VI. RESULTS

Surface scattering strengths, S_s, were computed using Eq. (5). The results are shown in Table I. The mean and standard deviation of S_s are given in Table II.

It has been found that Lambert's law

$$S_s = K + 10 \log \sin^2\theta$$

in optics is also a good model for describing backscattering of sound from rough sea bottoms.[8] Because the skeletal layer is somewhat analogous to a rough sea bottom, we used this model to formulate the following equation

$$S_s = S_o + B \log f + C \log \sin \theta, \quad f \text{ in kHz}, \tag{6}$$

Table I. Measured under-ice surface backscattering strength in decibels.

Set	Grazing Angle θ (deg)	Measured Values of S_s (dB) Frequency (kHz) 100	145	200	300
Field #1	15	-34.4	-29.9	-25.1	-21.2
	20	-31.2	-27.4	-25.7	-18.5
	30	-28.5	-25.4	-22.9	-17.5
	45	-28.3	-21.2	-19.7	-14.6
Field #2	10	-44.2	-38.9	-33.1	-24.6
	15	-37.9	-38.8	-34.4	-24.4
	20	-35.9	-28.6	-25.9	-21.8
	30	-33.9	-29.4	-25.2	-15.3
	45	-31.9	-22.2	-23.8	-18.6
Lab #2*	10	-39.9	-38.2	-29.0	-25.6
	15	-33.8	-28.2	-25.5	-20.1
	20	-27.0	-22.5	-17.9	-15.1
	30	-18.7	-16.4	-19.4	-12.8
	45	-25.8	-16.0	-17.5	-8.7
Lab #3	10	-47.8	-39.3	-31.8	-25.3
	15	-35.1	-33.9	-28.2	-20.2
	20	-29.9	-25.5	-20.6	-18.2
	30	-29.6	-25.6	-24.4	-15.2
	45	-26.0	-24.8	-18.4	-----
Lab #4	10	-31.1	-22.9	-25.1	-15.5
	15	-21.0	-21.7	-14.0	-13.2
	20	-25.8	-13.9	-10.9	-15.5
	30	-22.3	-16.8	-16.5	-14.6
	45	-19.1	-15.5	-18.5	-----
Lab #5	10	-21.8	-21.7	-21.8	-20.7
	15	-22.8	-21.0	-16.9	-17.0
	20	-27.4	-22.8	-20.5	-14.2
	30	-22.5	-21.2	-16.2	-19.2
	45	-----	-22.9	-19.1	-12.1
Lab #6	10	-26.8	-26.7	-18.1	-17.9
	15	-27.7	-18.0	-14.7	-16.9
	20	-22.3	-18.0	-15.7	-15.2
	30	-18.3	-25.2	-16.8	-12.5
	45	-22.7	-18.9	-14.9	-10.8

-- indicates no data.

*Laboratory set 1 was made with the transducer in mode 1, and was not used.

Table II. Mean and standard deviation of S_s values in Table I.

Grazing Angle θ	Frequency (kHz) 100		145		200		300	
	$\bar{S}_s$	σ	$\bar{S}_s$	σ	$\bar{S}_s$	σ	$\bar{S}_s$	σ
10	-35.27	6.67	-31.29	8.30	-26.15	6.02	-21.27	3.94
15	-30.39	6.57	-27.36	7.54	-22.69	7.68	-19.00	3.62
20	-28.22	4.61	-22.67	5.23	-19.03	5.30	-16.64	3.00
30	-24.83	5.92	-22.57	4.76	-20.20	3.91	-15.01	2.52
45	-25.30	4.48	-20.21	3.53	-18.84	2.68	-12.96	3.81

as a model for backscattering from an under-ice surface. The second term has been added to account for an observed frequency dependence. Variables S_o, B, and C are to be determined from experimental data.

Applying least-squares regression to the average S_s in Table II as a function of log f and log sin θ, we obtained -72, 25, and 15 for S_o, B, and C, respectively. The standard deviation of all the data in Table I from the S_s given by Eq. (6) was 5.25 dB.

The means of all data taken at 10°, 15°, 20°, 30°, and 45° are shown in Figure 9 along with plots of Eq. (6). It is clear that the equation is a good representation of the data.

A sample of Prudhoe Bay crude oil was provided by the ARCO refinery at Ferndale, Washington. The sample had a density of 0.87 g cm^{-3}. Its sound velocity of 1500 m s^{-1}, at seawater freezing temperatures, was 4% to 5% greater than that of the seawater. According to Snell's law, this indicates a critical grazing angle of ~17°. At any smaller angle, the acoustic energy incident on an oil surface would theoretically be reflected fully forward, and no energy would enter the oil layer to produce scattering from the ice above. In our laboratory tests, these effects were observed. At grazing angles greater than critical, the observed backscatter from the ice, through the oil layer, was about the same as when the oil was absent. The backscatter at small grazing angles depends mainly on the roughness of the surface and is much less from the smooth oil-water interface than from the rough ice-water interface.

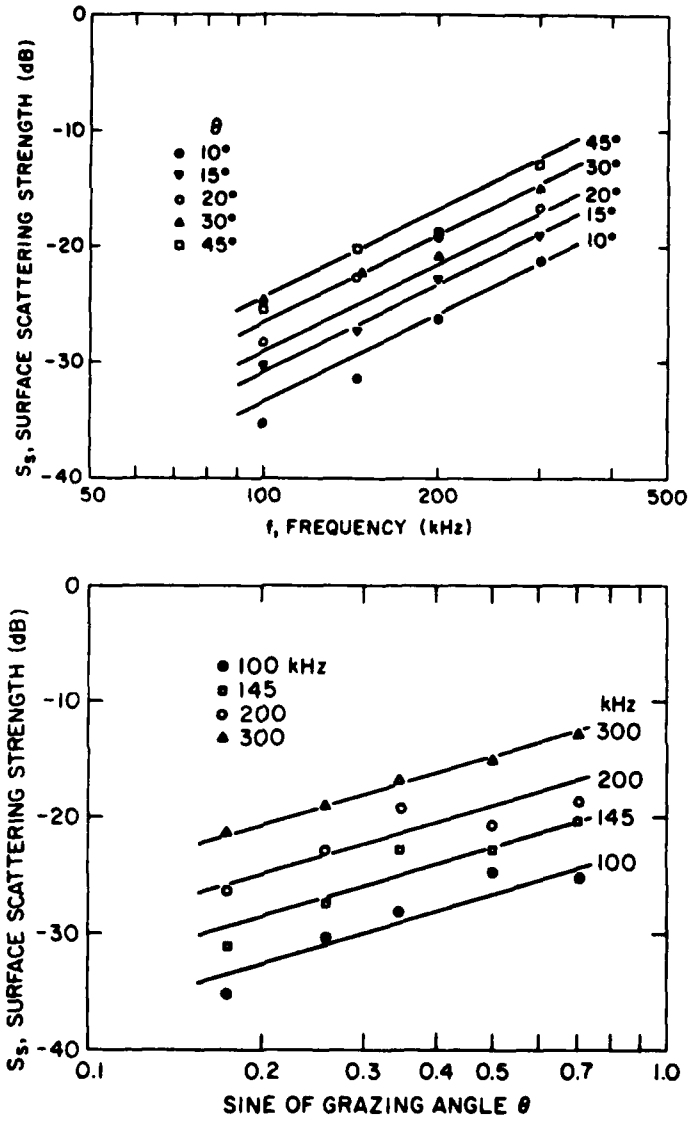

Figure 9. Average of measured S_s vs empirical equation $S_s = -72 + 25 \log f + 15 \log \sin \theta$.

VII. SAMPLE CALCULATIONS

Because acoustic differentiation between ice and oil appeared possible at low grazing angles, we next explored the question of whether the scattering strength of the ice surface is large enough, compared with ambient or system noise, to yield adequate survey ranges.

For this investigation, we used a 7.2 cm diameter circular piston transducer. The transducer characteristics and ambient conditions were as follows:

f, operating frequency, 200 kHz

α, absorption,[9,10] 0.0387 dB/m

beam width between -3 dB points, 6°

directivity index, 30 dB

efficiency, 50%, or -3 dB

Φ, equivalent two-way beamwidth, 0.157 rad

SL, source level,[11] 212.6 dB//μPa at 1 m

S_x, receiving sensitivity, -190 dBV/μPa

BW, receiving bandwidth, 20 kHz

τ, pulse length, 100 μs

DT, detection threshold, 10 dB

N_e, electronic noise, 6 nV/$\sqrt{\text{Hz}}$

N_a, ambient noise,[12] -2 dB//μPa in 1 Hz band.

For ambient and electronic noise, the total equivalent in-band acoustic noise level, NL, is

$$\text{Ambient NL} = N_a + 10 \log \text{BW} = 41 \text{ dB} ,$$

$$\text{Electronic NL} = 20 \log N_e + 10 \log \text{BW} - S_x = 68.6 \text{ dB} .$$

Therefore, the limiting noise contribution is from the electronics and we used the latter value for NL.

The applicable sonar equation in this case is

$$SL - 30 \log r - 2\alpha r + S_S + 10 \log \Phi + 10 \log \frac{c\tau}{2 \cos \theta} - NL = DT. \qquad (7)$$

In this equation, r represents the slant range and therefore

$$\frac{D}{r} = \sin \theta \ ,$$

where D is the depth of the sonar transducer.

Substituting this relationship into Eq. (6), we obtained:

$$S_S = S_O + B \log f + C \log \frac{D}{r} \ . \qquad (8)$$

Substituting Eq. (8) for S_S in (7), simplifying and rearranging terms, and noting $\cos \theta \simeq 1$ for small θ, we obtained

$$SL + B \log f + C \log D + 10 \log \Phi + 10 \log (c\tau/2) - NL - DT + S_O = (30 + C) \log r + 2\alpha r \ . \qquad (9)$$

We consider this equation, with S_O = -72 dB, to represent the 50% confidence level; for the 84% confidence level, the first term in the equation would be reduced by 1 σ (to -77.25 dB) and for the 97.75% confidence level, by 2 σ (to -82.5 dB), etc.

Applying regression values of B and C and the sample parameters given previously to Eq. (9) and solving for r, we obtained the following effective ranges for a transducer depth of 3 m at the specified confidence levels:

Confidence Level (%)	Detection Range (m)
50	149.3
84	125.1
98	103.6

These are quite usable distances. Within these ranges, for grazing angles less than critical, backscatter from the ice should show up well compared with that from the oil. Note that for these distances we are in fact extrapolating S_S to angles less than 10°. To compensate for the uncertainty resulting from extrapolation, a high nominal confidence level can be required if necessary.

In general, the design of an operational survey system would be relatively straightforward, once the parameters of the system are defined. The type of display system selected will influence the design of the beam pattern. A very narrow horizontal beam is desirable for good resolution at long range. However, this reduces the ensonified area and thus the backscattered energy. Similarly, a higher operating frequency will produce a higher S_s as well as higher sound absorption, each affecting the detection distance in opposite ways. Optimization studies of parameters such as these would be the next step toward the construction of an acoustic system for locating under-ice oil.

VIII. REFERENCES

1. J.L. Glaeser and G.P. Vance, "A study of the behavior of oil spills in the Arctic," Applied Technology Division, Office of Research and Development, U.S. Coast Guard, Washington, D.C., February 1971.

2. T.J. McMinn, "Crude oil behavior on arctic winter ice," Project 734108, Environmental and Transportation Technology Division, Office of Research and Development, U.S. Coast Guard, Washington, D.C., September 1972.

3. NORCO Engineering and Research, Ltd., "The interaction of crude oil with Arctic sea ice," Beaufort Sea Project, Dept. of Environment, Beaufort Sea Technical Report #27, December 1975.

4. L.W. Rosenegger, "The movement of oil under sea ice," Beaufort Sea Project, Dept. of Environment, Beaufort Sea Technical Report #28, December 1975.

5. P. Wadhams, "Sea ice morphology in the Beaufort Sea," Beaufort Sea Project, Dept. of Environment, Beaufort Sea Technical Report #36, December 1975.

6. E.R. Walker, "Oil, ice, & climate in the Beaufort Sea," Beaufort Sea Project, Dept. of Environment, Beaufort Sea Technical Report #35, December 1975.

7. E.L. Lewis, "Oil in sea ice," Institute of Ocean Sciences, Patricia Bay, Pacific Marine Science Report 76-12, June 1976 (unpublished manuscript).

8. R.J. Urick, Principles of Underwater Sound, 2nd ed. (McGraw-Hill, New York, 1975).

9. R.E. Francois and G.R. Garrison, "Sound absorption based on ocean measurements. Part I: Pure water and magnesium sulphate contributions," J. Acoust. Soc. Am. 72, 896-907 (1982).

10. R.E. Francois and G.R. Garrison, "Sound absorption based on ocean measurements. Part II: Boric acid contribution and equation for total absorption," J. Acoust. Soc. Am. 76, 1879-1890 (1982).

11. We assume that cavitation limits the output power to 0.326 W/cm^2 at zero depth or 13.2 W (acoustic) for the specified transducer.

12. Spectral level corrected for directivity index and hydrophone efficiency, thermal limit assumed.

END

DATE
FILMED

11 - 83

DTIC